Supplementary data for:

Biotechnological Model for Ubiquitous Mixed Petroleum- and Bio-Based Plastics Degradation and Upcycling into Bacterial Nanocellulose

Jeovan A. Araujo,*‡[a] George Taxeidis,‡[b] Everton Henrique da Silva Pereira,[a] Muhammad Azeem,[a] Brana Pantelic,[c] Sanja Jeremic,[c] Marijana Ponjavic,[c] Yuanyuan Chen,[a] Marija Mojicevic,*[a] Jasmina Nikodinovic-Runic,[c] Evangelos Topakas,[b] and Margaret Brennan Fournet[a]

[a] Centre for Polymer Sustainability, PRISM Research Institute, Technological University of the Shannon: Midlands Midwest, N37 HD68 Athlone, Ireland

[b] Biotechnology Laboratory, Department of Synthesis and Development of Industrial Processes, School of Chemical Engineering, National Technical University of Athens, Athens, Greece

[c] Institute of Molecular Genetics and Genetic Engineering, University of Belgrade, Vojvode Stepe 444a, 11000 Belgrade, Serbia

‡ Jeovan A. Araujo and George Taxeidis contributed equally to this work.

* Email: a00204000@student.tus.ie, araujojeovan@gmail.com (J.A.A.); marija.mojicevic@tus.ie (M.M.)

Note:

Number of pages: 17

Number of texts: 14

Number of figures: 9

Number of tables: 2

Table of Contents

Deleted: 3
Deleted: 3
Deleted: 4
Deleted: 5
Deleted: 6
Deleted: 6
Deleted: 7
Deleted: 8
Deleted: 9
Deleted: 9
Deleted: 9
Deleted: 10
Deleted: 11
Deleted: 11
Deleted: 12
Deleted: 15
Deleted: 15
Deleted: 16
Deleted: 17

Methods

Text S1: Method for model home composting bioaugmented with Bacillus sp. BPM12

Biodegradability of PET-TPS films was assessed in laboratory model compost during 10 weeks at 37 °C, according to a previously described protocol (Pantelic et al., 2021). The model composting system consisted of a commercial mixture of raw materials used for the cultivation of white button mushroom (80%, w/w) and universal soil for gardening and potting (20%, w/w), both obtained from ACS Garden (Belgrade, Serbia). Film samples weighing between 60–120 mg were rinsed with 70% EtOH and air dried, buried in compost (150 g) at a depth of 1 cm, in duplicates, and humidity was set up at approximately 50% with distilled water. Two types of compost were used: pristine non-treated compost and compost bioaugmented with *Bacillus* sp. BPM12 strain ($\log10^4$ cells/gram of compost). *Bacillus* sp. BPM12 grown overnight in LB medium (Luria Bertani, 10 $g \cdot L^{-1}$ tryptone, 5 $g \cdot L^{-1}$ yeast extract, 10 $g \cdot L^{-1}$ NaCl) kept at 180 rpm and 30 °C was used for inoculation, while 20% glycerol stocks were prepared and stored at -80 °C for continuous replenishment of model home bioaugmented composting. Samples were inspected weekly, when fresh aliquots of bacterial culture were added to bioaugmented compost, and distilled water was added to pristine compost, in order to maintain constant humidity. After 10 weeks of incubation, samples were removed, rinsed with 70% EtOH, air dried, and stored before further tests were carried out.

Text S2: Quantification of BHET, MHET, and TPA via HPLC analysis

The quantification of TPA, MHET, and BHET present in the degradation products released after enzymatic treatment was performed by constructing the calibration curves below (Fig. S1), which were based on the HPLC peak area (AUC) method.

Deleted: Fig. S1

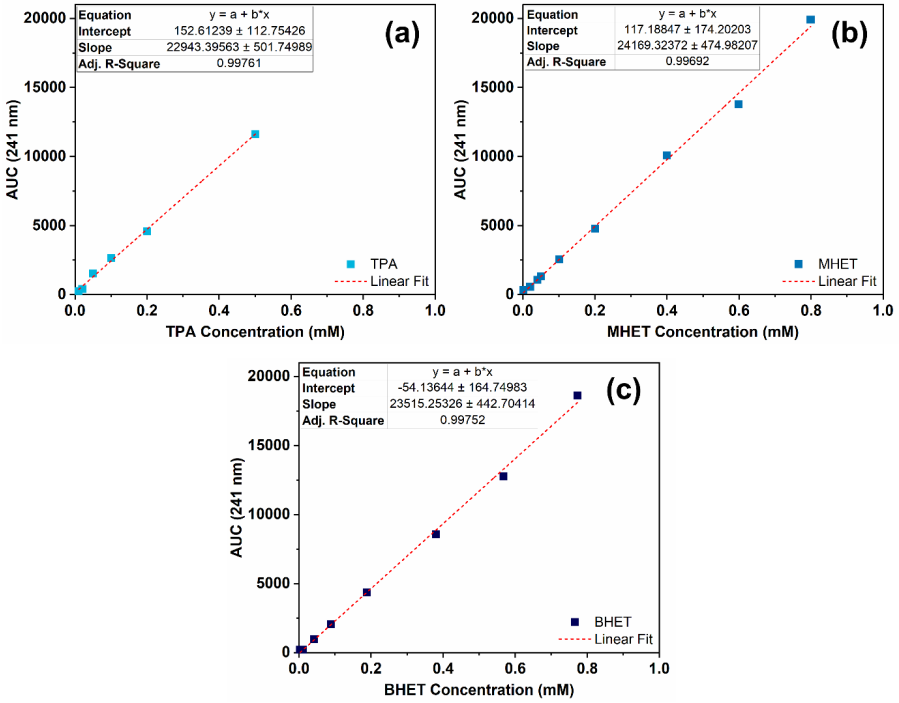

Fig. S1. Calibration curves used for HPLC quantification of (a) TPA, (b) MHET, and (c) BHET. Standard concentrations were used in the range of 0.01–0.8 mM. Inserts show the details related to the linear fit applied to each curve, including the goodness of fit (R^2).

Text S3: Quantification of reducing sugars via DNS colorimetric method

A calibration curve of the absorbance at 540 nm (a.u.) was plotted against the glucose concentration (mg·mL^{-1}), which was used as a standard (Fig. S2).

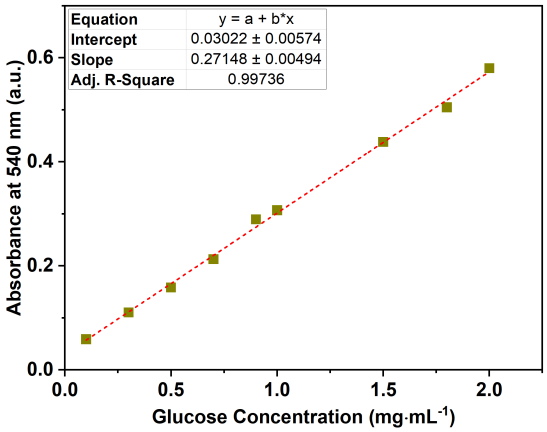

Fig. S2. Calibration curve used to determine the amount of reducing sugars via DNS method. The insert shows the details of the linear fit applied to the curve, including the goodness of fit (R^2).

Deleted: Fig. S2

Formatted: Font: Not Italic, Check spelling and grammar

Characterization

Text S4: Infrared spectrum of the starting TPS (model bioplastic)

The spectrum of neat TPS film (Fig. S3) has been previously examined elsewhere in the literature (Araujo et al., 2021). Thermoplastic potato starch (TPS) was used as a model bioplastic in the mixed (petro-bio)plastic materials. The spectrum of TPS showed a strong band at 1758 cm^{-1} attributed to the stretching of C=O group that might have resulted from the plasticization process of starch. The typical band observed at 1454 cm^{-1} was attributed to C–H bending vibrations, while bands at 1184 and 1044 cm^{-1} were due to changes in the C–O and C–O–H stretching vibrations.

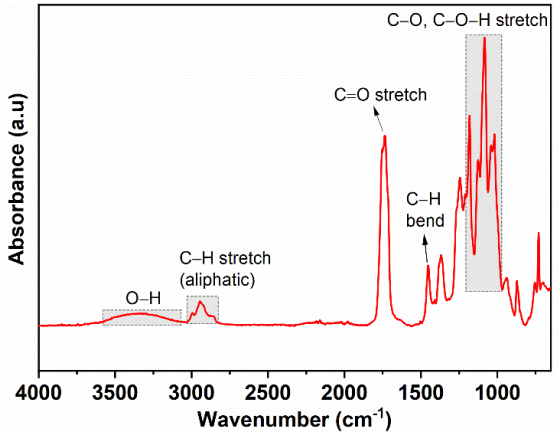

Fig. S3. FTIR spectrum of TPS in the wavenumber range from 4000 to 650 cm^{-1}.

Deleted: Fig. S3

Formatted: Font: Not Italic, Check spelling and grammar

Text S5: Thermal properties of the mixed (petro-bio)plastic films

The thermal properties of the mixed (petro-bio)plastic materials with varying bioplastic content were evaluated by DSC (Fig. S4).

Deleted: Fig. S4

Formatted: Font: Not Italic, Check spelling and grammar

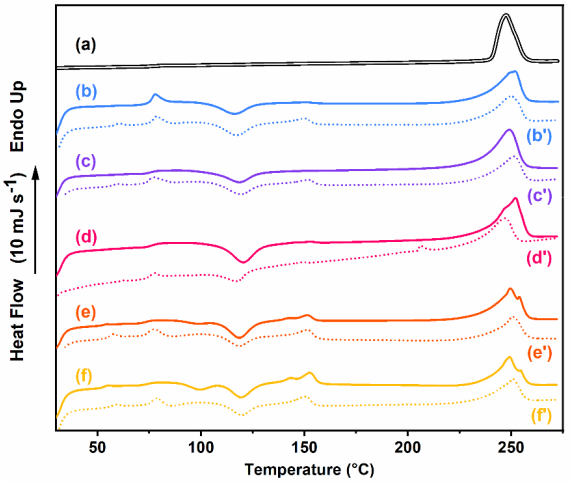

Fig. S4. First heating scan from DSC curves of (a) PET pellets, (b, b') neat PET, (c, c') PETTPS5, (d, d') PET-TPS10, (e, e') PET-TPS30, and (f, f') PET-TPS40 materials. Double line, starting PET pellets used as received; solid lines, extruded mixed (petro-bio)plastic films; dashed lines, powder samples obtained from the extruded films after milling process.

Table S1. Thermal properties of the starting PET pellets, film and powder PET and PET-TPS samples calculated from the first heating DSC scan.

Sample	Processing	Sample form	Melting enthalpy ($J.g^{-1}$)	Crystallinity (%)
PET	none (used as received)	pellet	72.8	52.0
PET	hot-melt extrusion	film	53.6	38.3
PET-TPS5	hot-melt extrusion	film	52.2	37.3
PET-TPS10	hot-melt extrusion	film	44.2	31.5
PET-TPS30	hot-melt extrusion	film	38.5	27.5
PET-TPS40	hot-melt extrusion	film	30.5	21.8
PET	extrusion + milling	powder	39.1	27.9
PET-TPS5	extrusion + milling	powder	37.4	26.7
PET-TPS10	extrusion + milling	powder	32.8	23.4
PET-TPS30	extrusion + milling	powder	31.6	22.6

PET-TPS40	extrusion + milling	powder	28.5	20.4

Text S6: Mechanical properties of the mixed (petro-bio)plastic films

Being one of the most significant inherent properties to describe the mechanical behavior of materials, E enabled the measurement of the mixed PET-TPS films' elasticity or their ability to withstand a given load with minimum extension, whereas σ measured the films' ability to withstand a load without permanently deforming or breaking. The average E and σ results are summarized in Error! Reference source not found.. The extruded neat PET film showed an average E of 2239 ± 105 MPa, and σ of 38 ± 5 MPa, which are typical values for PET films (Gupta et al., 2009). In comparison to that of neat PET, it was demonstrated that the elasticity was not expressively affected when TPS was mixed at 5 and 10 wt.%, in which E decreased to 2093 ± 215 MPa (p = 0.212) and 2028 ± 61 MPa (p = 0.053) in the PET-TPS5 and PET-TPS10 films, respectively. On the other hand, a significant deterioration in stiffness was demonstrated by a decline in E to 1985 ± 135 MPa (p = 0.050) in the PET-TPS30 film, and a subsequent decrease to 1628 ± 83 MPa (p = 0.002) in the PET-TPS40 sample. Interestingly, the increasing TPS content in the mixed (petro-bio)plastic materials significantly deteriorated the hardness of the compounded PET-TPS films in comparison to that of neat PET. The average σ values declined to 21 ± 1 MPa (p = 0.002), 21 ± 2 MPa (p = 0.003), 19 ± 3 MPa (p = 0.003), and 13 ± 2 MPa (p = 0.001) in the PET-TPS5, PET-TPS10, PET-TPS30, and PET-TPS40 samples, respectively.

Deleted: Table 1.

Biodegradation of the mixed PET-TPS materials

Text S7: Home composting bioaugmented with Bacillus sp. BPM12

Home composting is considered an environmentally beneficial, low-tech, garden technique, then we first developed a model home composting system bioaugmented with *Bacillus* sp. BPM12 to evaluate the biodegradation of mixed PET-TPS materials. PET-TPS samples were incubated for a period of ten weeks at 37 °C, and post-composting samples were further characterized by FTIR (Fig. S5) and SEM (Fig. S6) analysis.

Text S8: Infrared spectra of post-composting neat PET vs. PET-TPS40 film

FTIR spectra of post-composting neat PET and PET-TPS40 films in pristine and bioaugmented conditions are presented in Fig. S5. No significant change in the structure of neat PET film was observed in the FTIR spectra, while the disappearance of the band at 1754 cm^{-1} in the spectrum of the PET-TPS40 films incubated in the bioaugmented compost indicated the removal of TPS from the mixed (petro-bio)plastic film. This was attributed to the slight increase in the biodegradation of PET-TPS40 in bioaugmented compost (4.1%) compared to pristine compost (3.4%), which implied that TPS can be degraded from the mixed plastic under these incubation conditions. Despite no remarkable change was detected in the structure of the neat PET film, a minor change in the *CI* value related to the intensity of the carbonyl band at 1712 cm^{-1} was observed, while this change was evident for the mixed PET-TPS40 film, in which the *CI* decreased from 2.51 to 2.39.

Deleted: Fig. S5

Deleted: Fig. S6

Formatted: Font: Not Italic, Check spelling and grammar

Formatted: Font: Not Italic, Check spelling and grammar

Deleted: Fig. S5

Formatted: Font: Not Italic, Check spelling and grammar

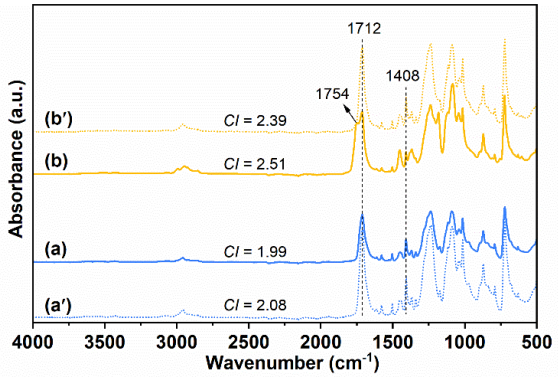

Fig. S5. FTIR spectra of post-composting (a) neat PET and (b) PET-TPS40 films in pristine compost compared to (a') neat PET and (b') PET-TPS40 films bioaugmented with *Bacillus* sp. BPM12. The carbonyl index (*CI*) is the ratio between the intensity of the bands at 1712 and 1408 cm^{-1}.

Text S9: Microstructure analysis of post-composting neat PET vs. PET-TPS40 film

The biodegradation of the mixed PET-TPS films over bioaugmented compost with Bacillus sp. BPM12 was also investigated by SEM analysis (Fig. S6). No significant changes were observed on the surface of the neat PET samples treated with pristine compost (Fig. S6, a') and bioaugmented compost (Fig. S6, a'') in comparison to that of the non-treated PET film (Fig. S6, a). On the other hand, the micrograph of the mixed PET-TPS40 film treated with bioaugmented compost (Fig. S6, b'') showed some signs of deterioration, while such changes were less pronounced in the PET-TPS40 sample without the BPM12 treatment (Fig. S6, b') in contrast to that of the starting PET-TPS40 film (Fig. S6, b).

Deleted: Fig. S6
Formatted: Font: Not Italic, Check spelling and grammar
Deleted: Fig. S6
Formatted: Font: Not Italic, Check spelling and grammar
Deleted: Fig. S6
Formatted: Font: Not Italic, Check spelling and grammar
Deleted: Fig. S6
Formatted: Font: Not Italic, Check spelling and grammar
Deleted: Fig. S6
Formatted: Font: Not Italic, Check spelling and grammar
Deleted: Fig. S6
Deleted: Fig. S6
Formatted: Font: Not Italic, Check spelling and grammar
Formatted: Font: Not Italic, Check spelling and grammar

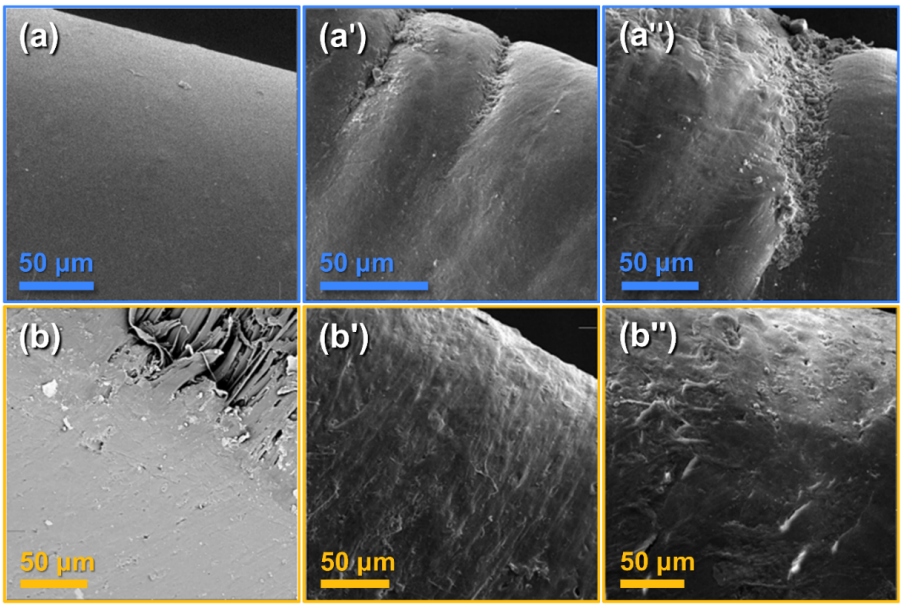

Fig. S6. SEM images of the neat PET and PET-TPS40 films before and after composting: (a) non-treated PET, (a') PET treated with pristine compost, and (a'') PET treated with *Bacillus* sp. BPM12 bioaugmented compost; (b) non-treated PET-TPS40, (b') PET-TPS40 treated with pristine compost, and (b'') PET-TPS40 treated with *Bacillus* sp. BPM12 bioaugmented compost.

Text S10: Enzymatic degradation study

Although various enzymes have also shown the ability to degrade PET down to its intermediates (*i.e.* BHET, MHET, and TPA), the extent of their use for biodegradation has been linked to limited enzymatic activity due to various technical factors such as thermal instability around the polymer T_g, and highly influenced by hydrophobicity, structure, and crystallinity of the material (Maurya et al., 2020).

Text S11: Enzymatic degradation at 30 °C

The degradation of the mixed PET-TPS materials was initially studied at 30 °C (Fig. S7a). The enzymatic decomposition of samples occurred mostly due to AMY action, an expected result considering the low activity of LCC^{ICCG} at this temperature (Shirke et al., 2018). Enzymatic depolymerization was below 20% for all samples in the reaction systems containing AMY and LCC^{ICCG}/AMY, except when the PET-TPS40 material was degraded by LCC^{ICCG}/AMY and a maximum depolymerization of 30.1 ± 0.9% was observed. The enzymatic degradation of PET-TPS films was further confirmed by detecting and quantifying degradation products from the hydrolysis reaction, from which TPA, MHET, and BHET were detected as PET intermediate products. As expected, the total amount of PET intermediates released was very low at 30 °C, around only 0.01 $mg{\cdot}mL^{-1}$, or in some cases not detected at all (Fig. S7b). This clearly indicated that this temperature is not favorable for any enzymatic treatment investigated for the mixed PET-TPS plastic. Nevertheless, PET-TPS40 had the highest amount of reducing sugars among all degraded films at 30 °C (Fig. S7c), increasing from 1.43 ± 0.1 $mg{\cdot}mL^{-1}$ after AMY treatment to 3.0 ± 0.2 $mg{\cdot}mL^{-1}$ when both enzymes were combined in the LCC^{ICCG}/AMY treatment, which indicated a synergistic decomposition effect. This finding was clearly shown by DS = 2.0 for PET-TPS40, which was the highest value observed at 30 °C (Fig. S7d).

Deleted: Fig. S7

Formatted: Font: Not Italic, Check spelling and grammar

Deleted: Fig. S7

Formatted: Font: Not Italic, Check spelling and grammar

Deleted: Fig. S7

Formatted: Font: Not Italic, Check spelling and grammar

Deleted: Fig. S7

Formatted: Font: Not Italic, Check spelling and grammar

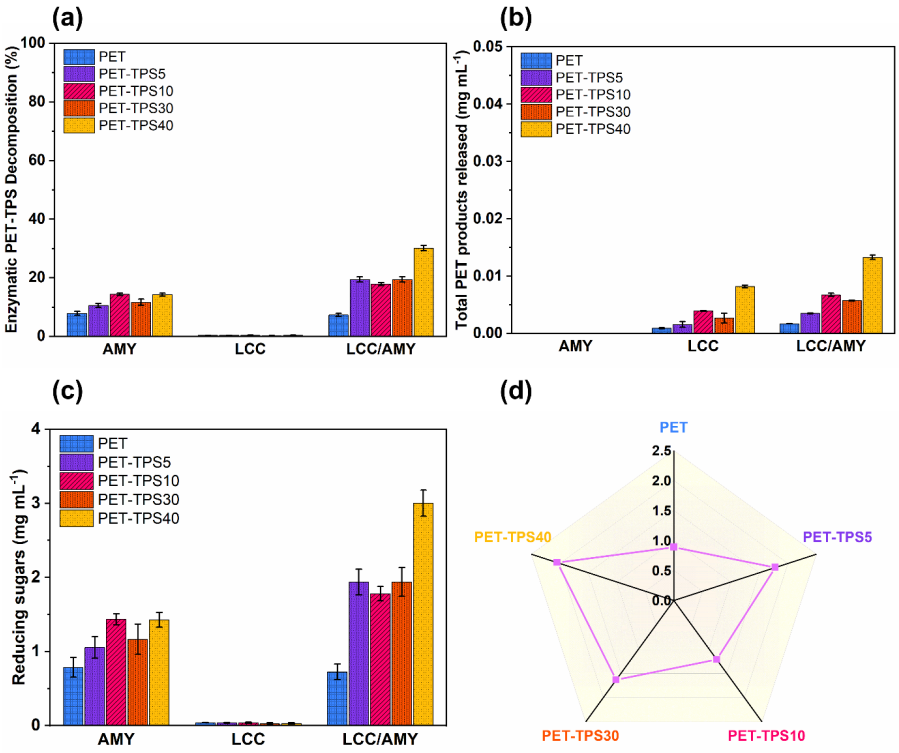

Fig. S7. Enzymatic degradation study on the mixed PET-TPS films using AMY, LCC^{ICCG}, and LCC^{ICCG}/AMY at 30 °C: (a) Enzymatic decomposition (%) calculated from the total degradation products (BHET, MHET, TPA, and reducing sugars); (b) Total PET products released detected by HPLC analysis; (c) Reducing sugars detected via the DNS method; and (d) Comparison of degree of synergism (DS) for the different mixed PET-TPS samples. DS was calculated from the total decomposition by LCC^{ICCG}/AMY in relation to each individual enzymatic treatment. Reactions were carried out for four days under constant agitation (1200 rpm) using 30 µg of AMY, 0.12 µg of LCC^{ICCG}, or a combination of both enzymes in 0.1 M phosphate buffer, pH = 7. The concentration of 100% PET-TPS degradation products is equivalent to 10 mg·mL^{-1}. Tests were carried out in triplicate; error bars represent the standard deviation of the mean values.

Text S12: Enzymatic degradation at 50 °C

Then, the degradation reaction of the mixed PET-TPS films was studied at 50 °C. As it can be clearly seen in Fig. S8a, the overall performance of the enzymatic treatments was improved with the temperature increase, indicating that both AMY and LCC^{ICCG} enzymes are active at 50 °C. The improved degradation was attributed to the activation of LCC^{ICCG}, as demonstrated by a 15% depolymerization of neat PET film treated with only LCC^{ICCG}. Moreover, the combined LCC^{ICCG}/AMY treatment synergistically improved the enzymatic decomposition of the PET-TPS films, with depolymerization rates up to 31%. This was supported by an increase in the total concentration of TPA, MHET, and BHET released from PET-TPS films after the LCC^{ICCG}/AMY treatment at 50 °C, which ranged from 1.9 to 2.3 mg·mL^{-1} (Fig. S8b). Reducing sugars were detected in all treatment scenarios at 50 °C, however this was limited to only 1.3 mg·mL^{-1} was detected for PET-TPS40 treated with AMY alone (Fig. S8c). As suggested above, increased enzymatic depolymerization was correlated with the enzymatic degradation synergy for the mixed PET-TPS films, particularly for the PET-TPS10 sample that showed a DS = 1.5 (Fig. S8d).

Deleted: Fig. S8

Deleted: Fig. S8

Deleted: Fig. S8

Deleted: Fig. S8

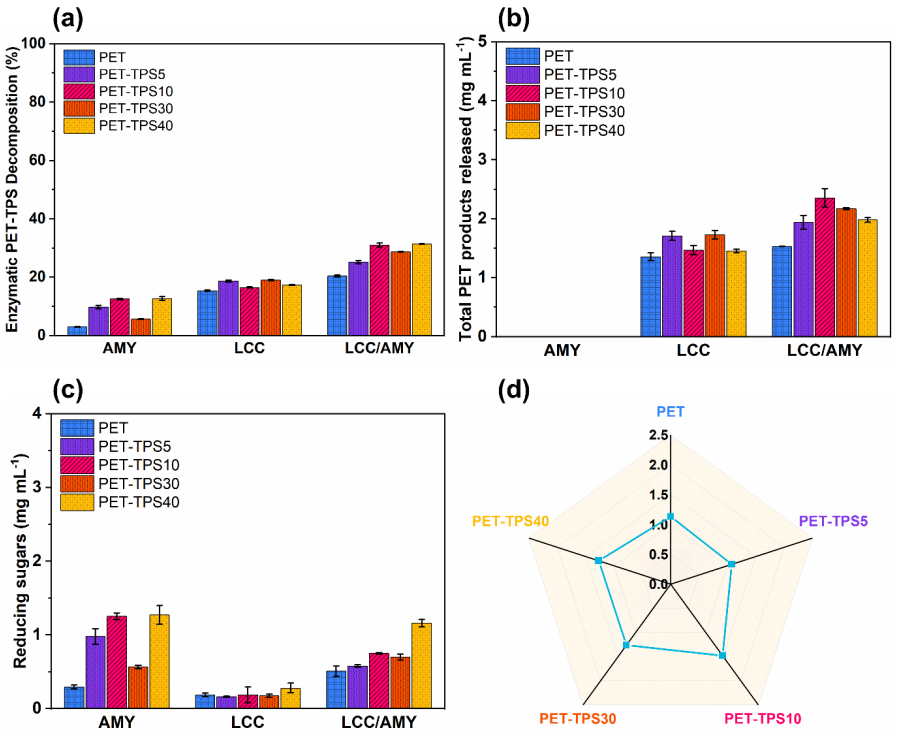

Fig. S8. Enzymatic degradation study on the mixed PET-TPS films using AMY, LCC^{ICCG}, and LCC^{ICCG}/AMY at 50 °C: (a) Enzymatic decomposition (%) calculated from the total degradation products (BHET, MHET, TPA, and reducing sugars); (b) Total PET products released detected by HPLC analysis; (c) Reducing sugars detected via the DNS method; and (d) Comparison of degree of synergism (DS) for the different mixed PET-TPS samples. DS was calculated from the total decomposition by LCC^{ICCG}/AMY in relation to each individual enzymatic treatment. Reactions were carried out for four days under constant agitation (1200 rpm) using 30 μg of AMY, 0.12 μg of LCC^{ICCG}, or a combination of both enzymes in 0.1 M phosphate buffer, pH = 7. The concentration of 100% PET-TPS degradation products is equivalent to 10 mg·mL^{-1}. Tests were carried out in triplicate; error bars represent the standard deviation of the mean values.

Bio-upcycling of mixed PET-TPS hydrolysates into bacterial nanocellulose (BNC)

Text S13: Infrared spectrum and visual appearance of the produced BNC

The harvested BNC films were air-dried appropriately at 60 °C, and cut into tapes before FTIR analysis (Fig. S9). For comparison purposes, two BNC samples were selected: (a) BNC obtained from the control HS medium, and (b) BNC grown from the mixed PET-TPS40 hydrolysates obtained after the synergetic degradation by the LCC^{ICCG}/AMY treatment. Both samples are visually similar with subtle color differences. FTIR spectra of both BNC samples from (a') control HS medium and (b') PET-TPS40 hydrolysates showed analogous characteristic bands, including a broad O–H stretching vibration centered at 3330 cm^{-1}, C–H aliphatic stretching between 2985–2850 cm^{-1}, O–H bending at 1626 cm^{-1}, CH_2 bending at 1427 cm^{-1}, C–O stretching vibrations at 1270, 1240, and 1160 cm^{-1}, and C–O–C pyranose ring skeletal stretching vibrations at 1052 and 1028 cm^{-1} (Molina-Ramírez et al., 2018; Rozenberga et al., 2016).

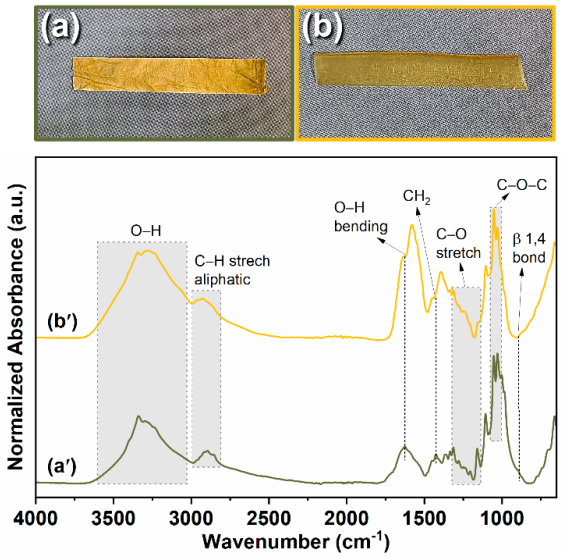

Fig. S9. Digital images (top) and FTIR spectra (bottom) of the BNC produced from (a, a') HS medium used as glucose-supplemented control and (b, b') PET-TPS40 hydrolysates obtained from the LCC^{ICCG}/AMY enzymatic treatment at 50 °C.

Deleted: Fig. S9

Formatted: Font: Not Italic, Check spelling and grammar

Text S14: Estimation of the mixed PET-TPS plastic conversion to BNC

The conversion of mixed (petro-bio)plastic to BNC was estimated by taking the amount of BNC produced (g) after each enzymatic treatment in relation to the initial amount of mixed plastic substrate (g) from which the hydrolysates were obtained via enzymatic degradation. The conversion expressed in percentage (%) is measured as g of BNC per g of PET-TPS substrate used, and the results are presented below in **Table S2**.

Table S2. Conversion of mixed PET-TPS hydrolysates to BNC following AMY, LCC, and LCC^{ICCG}/AMY enzymatic treatments at 50 °C.

Sample	Amount of plastic substrate (g)	Conversion to BNC (%)		
		AMY	LCC	LCC/AMY
PET	1	0.00%	0.00%	0.00%
PET-TPS5	1	0.00%	0.00%	0.41%
PET-TPS10	1	0.38%	0.28%	0.58%
PET-TPS30	1	0.38%	0.27%	0.53%
PET-TPS40	1	0.41%	0.34%	0.58%

References

Araujo, J.A., Cortese, Y.J., Mojicevic, M., Brennan Fournet, M., Chen, Y., 2021. Composite Films of Thermoplastic Starch and $CaCl_2$ Extracted from Eggshells for Extending Food Shelf-Life. Polysaccharides 2, 677–690. https://doi.org/10.3390/polysaccharides2030041

Maurya, A., Bhattacharya, A., Khare, S.K., 2020. Enzymatic Remediation of Polyethylene Terephthalate (PET)–Based Polymers for Effective Management of Plastic Wastes: An Overview. Front Bioeng Biotechnol 8. https://doi.org/10.3389/fbioe.2020.602325

Molina-Ramírez, C., Enciso, C., Torres-Taborda, M., Zuluaga, R., Gañán, P., Rojas, O.J., Castro, C., 2018. Effects of alternative energy sources on bacterial cellulose characteristics produced by Komagataeibacter medellinensis. Int J Biol Macromol 117, 735–741. https://doi.org/10.1016/j.ijbiomac.2018.05.195

Pantelic, B., Ponjavic, M., Jankovic, V., Aleksic, I., Stevanovic, S., Murray, J., Fournet, M.B., Nikodinovic-Runic, J., 2021. Upcycling Biodegradable PVA/Starch Film to a Bacterial Biopigment and Biopolymer. Polymers (Basel). https://doi.org/10.3390/polym13213692

Rozenberga, L., Skute, M., Belkova, L., Sable, I., Vikele, L., Semjonovs, P., Saka, M., Ruklisha, M., Paegle, L., 2016. Characterisation of films and nanopaper obtained from cellulose synthesised by acetic acid bacteria. Carbohydr Polym 144, 33–40. https://doi.org/10.1016/j.carbpol.2016.02.025

Shirke, A.N., White, C., Englaender, J.A., Zwarycz, A., Butterfoss, G.L., Linhardt, R.J., Gross, R.A., 2018. Stabilizing Leaf and Branch Compost Cutinase (LCC) with Glycosylation: Mechanism and Effect on PET Hydrolysis. Biochemistry 57, 1190–1200. https://doi.org/10.1021/acs.biochem.7b01189